Test of the Moisture Mass Conservation in LM

Günther Doms

Deutscher Wetterdienst, P.O.Box 100465, 63004 Offenbach a.M., Germany

1 Background

The model equations of LM use a prognostic equation for the pressure perturbation, which is derived from the continuity equation for total mass and includes some additional approximations. Consequently, the model lacks an explicit control of conservation properties. Also, the budget equation for the water species are numerically solved in advection form, and thus the conservation of water mass cannot be guaranteed (see Part 1 of the LM Documentation).

From a physical point of view, it is of course useful to construct a numerical model around conservation principles for the basic variables. E.g., water mass conservation is important to avoid artificial sources and sinks in the hydrological cycle, and total mass conservation is required to reproduce correctly the hydrostatic pressure field. On the other hand, mass conserving numerical schemes do not necessarily guarantee an accurate solution. For instance, the application of a flux-form upstream scheme for the budget equations will always give a mass conserving solution, but in many circumstances the solution will be too smooth to be of any practical use.

Besides the use of the pressure equation and the application of the advective form, there are several other factors which contribute to an artificial loss and gain of total and water mass.

- The continuity equation is used to derive a prognostic equation for pressure

$$\frac{\partial \rho}{\partial t} + \nabla \cdot (\rho \mathbf{v}) = 0 \quad \rightarrow \quad \frac{dp}{dt} = -(c_{pd}/c_{vd}) p \nabla \cdot \mathbf{v} + (c_{pd}/c_{vd} - 1) Q_h \,, \tag{1}$$

  where Q_h is the diabatic heating term appearing in the prognostic equation for temperature T. In the model equations, however, this term in neglected in (1). Thus, by reconstructing the continuity equation from the model equations, an artificial source term related to diabatic heating will arise.

- Additional errors result from numerical discretization (e.g. 3-d advection in the vicinity of steep topography) and the utilization of numerical filters (e.g. horizontal diffusion).

- All relaxation terms can act as sources or sinks of mass. Examples are the lateral boundary relaxation technique, the Rayleigh damping layers at the model top or the nudging analysis scheme.

- The application of a zero boundary condition for the vertical velocity ($w = 0$) at the lower boundary is a problem. Since the velocity is defined to be the barycentric velocity, w will not be zero if there is precipitation fallout or evaporation (dew formation) at the ground.

Even if the equations are not applied in conservation form, an accurate non-conservative scheme can in principle closely satisfy conservation. In this paper we address the question of how accurate is the LM solution is in practice.

2 Budget Equations

In order to assess the water mass conservation, the rate of change within a vertical column over a gridpoint will be calculated using the model predicted values of total air density ρ and the specific mass fractions q_k with $k = v$ (water vapour), $k = c$ (cloud water), $k = i$ (cloud ice), $k = r$ (rain) and $k = s$ (snow) at time level n and $n + 1$, resulting in a rate of change per time step. This rate will then be compared with the change that would result if the mass-budget would be calculated based on the corresponding 'exact' budget equations.

To do so, we start with the local differential form of the LM budget equations for the water species ($k = v, c, i, r, s$):

$$\frac{\partial \rho q_k}{\partial t} + \nabla \cdot (\rho q_k \mathbf{v}) + \frac{\partial F_k}{\partial z} - \frac{\partial P_k}{\partial z} = S_k \,, \tag{2}$$

where $\mathbf{v}$ is the barycentric wind vector and S_k are source rates. P_k denotes the precipitation flux (nonzero only for rain and snow) and F_k is the turbulent flux of species k (nonzero only for water vapour, cloud water and cloud ice). Adding the equations (2) for all water species results in the budget equation for the total water mass fraction $q = \sum_k q_k$:

$$\frac{\partial \rho q}{\partial t} + \nabla \cdot (\rho q \mathbf{v}) + \frac{\partial (F_v + F_c + F_i)}{\partial z} - \frac{\partial (P_r + P_s)}{\partial z} = 0 \,. \tag{3}$$

The gridpoint-column budget is obtained by integrating (3) over a control volume $V_c = A_c(z_t - z_s)$, where z_t denotes the height of the model domain top, z_s is the topographical height of the surface, and $A_c = a^2 cos\varphi \Delta\lambda \Delta\varphi$ is the discrete horizontal area element represented by a gridpoint. In this way, local errors can be considered for each column, and – on the other hand – a large-scale budget is easily obtained by summing up the columnwise budgets for an arbitrary subdomain. Defining the column water mass per unit area as

$$m_w = \frac{1}{A_c} \int \rho q dV_c \quad \textit{total water per unit area} \tag{4}$$

and using (3), the semi-discretized column water mass budget equation may be derived:

$$\frac{dm_w}{dt} = -\sum_l \nabla_h \cdot (\rho q \mathbf{v}_h)_l \Delta z_l + F_s^v - P \,. \tag{5}$$

Here, $\mathbf{v}_h$ denotes the horizontal wind vector. The flux divergence term is evaluated for each model layer l with thickness Δz_l and then the sum over all layers is calculated. F_s^v denotes the surface flux of water vapour (positive for evaporation, negative for dew formation at the ground; turbulent transports of cloud water and cloud ice at the ground have been neglected), and P denotes the total precipitation flux at the ground (rain and snow).

An additional assumption made for (5) is that the barycentric vertical velocity vanishes at the top and bottom of a column. At the lower boundary, however, w is zero only when both F_s^v and P are zero – which usually is not the case. Taking the impact of vapour diffusion and precipitation fallout into account more precisely would result in a correction factor ρ_a/ρ for the terms F_s^v and P in the budget equation (5), where ρ_a denotes the density of dry air. Since this factor is very close to 1, we will neglect this effect in the present context. A detailed investigation of the use of continuity equations for water species and on the impact of the lower boundary condition for the barycentric vertical velocity on the total mass budget has been recently presented by Wacker and Herbert (2003).

We can now proceed to check the water mass budget of the model by evaluating the rate of change at a timestep t_n as given by the right hand side of (5) and comparing this result

with the rate of change as resulting from the model integration. The latter rate will be denoted as $(dm_w/dt)_M$ and is evaluated as $(m_w(t_{n+1}) - m_w(t_n))/\Delta t$, using the predicted model variables to calculate m_w at time level $n+1$ and n (Δt is the time step). Because of model and discretization errors, the model predicted value for the change in m_w will differ form the 'exact' mass-conserving rate of change (5) by a residuum value R:

$$\left(\frac{dm_w}{dt}\right)_M = \frac{dm_w}{dt} + R. \tag{6}$$

Whenever the residuum R is positive, the model predicted change in water mass is larger than the mass-conserving change would prescribe – that is there is an artificial erroneous gain of mass. Values $R < 0$ indicate an artificial loss of water mass. Equation (6) can also be integrated in time resulting in a column mass-budget for a certain time period. Denoting the start and end time of an arbitrary time period by t_0 (with time step index n_0) and t_1 (with time step index n_1), respectively, yields

$$m_w(t_1)_M - m_w(t_0)_M = \sum_{n_0}^{n_1}(-Div + F_s^v - P)_n \Delta t + \sum_{n_0}^{n_1} R_n \Delta t. \tag{7}$$

The term Div on the right hand side denotes the column integrated water mass divergence as given by the first term on the rhs of Eq. (5). We use second-order centered differences to evaluate Div such that outflow from one cell is counted as inflow to the corresponding neighboring cell. Thus, it is easy to obtain the budget (7) also for an arbitrary model subdomain by simply adding over all gridpoints within the subdomain. All flux-contributions from Div will cancel except for the outer boundaries where they define the net lateral outflow ($Div > 0$) or inflow ($Div < 0$). All components to calculate the mass budget are available by standard model output (i.e. the vertically integrated water mass m_w at output time and the time-integrated values of Div, F_s^v and P), the residuum R can thus be calculated in a simple post-processing program.

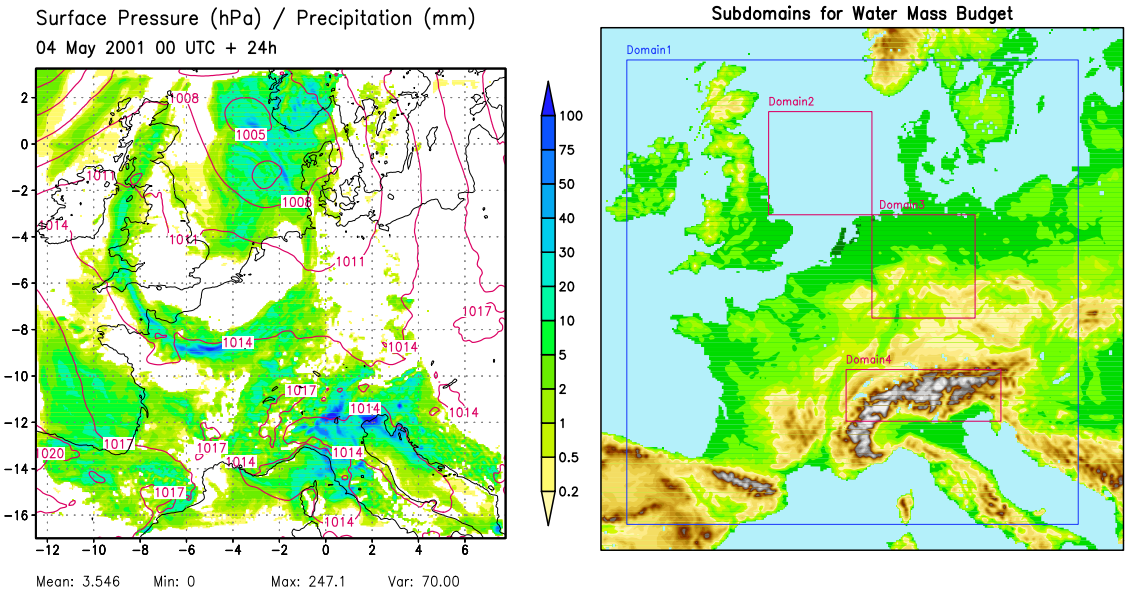

Figure 1: Left: 24-h LM-forecast starting from 4 May 2002 00 UTC; mean sea-level pressure (isolines) and 24-h accumulated total precipitation (shaded). Right: 4 subdomains chosen to calculate area-average water mass budgets.

3 Water Mass Budget Results

As a first (arbitrary) test case to calculate the LM water mass budget we have chosen a 48-h forecast starting on 4 May 2002 00 UTC. The initial conditions have been interpolated from the corresponding GME analysis. The weather situation (see Fig. 1, left) is characterized by two weak low pressure systems over the North Sea and over northern Italy. Whereas the northern system is associated with mostly stratiform precipitation, the southern system is of convective nature with heavy thunderstorms along the southern Alpine ridge.

Fig. 1 (right) illustrates the position of four different subdomains where we calculate hourly area average water mass budgets according to (7) – normalized by the area of the subdomains in order to avoid too large numbers. Domain 1 corresponds closely to the total model domain but excludes the lateral boundary relaxation zone in order to avoid errors from the boundary treatment. Domain 2 has been chosen over the North Sea, where errors resulting from sloping model surfaces due to topography will not occur. Domain 3 covers the northern parts of Germany, the impact from topography is expected to be noticeable but quite small. Finally, Domain 4 is positioned directly over the Alps. Here we expect the largest discretization errors related to very steep topography.

We first look at the results for subdomain 2 (North Sea) as shown in Figure 2 (left). Except for the first 12h of integration, the contributions of surface evaporation (yellow) and precipitation (red) balance approximately. Consequently, the total rate of change in water mass (black) closely follows the change due to net inflow (blue). During the first and last 15 hours of integration, the model predicted change in water mass (black line) follows the mass-conserving change (green) as calculated from (5) almost exactly – the residuum (purple) is practically zero. However, in the 15-33h forecast range (mostly during night) a noticeable positive deviation of the residuum can be noticed. The artificial mass gain rate is up to 5% of the total water mass change. Since the physical forcing for this subdomain is relatively small and errors due to topography can be excluded, the reason for this error might be attributed to the discretization of transport terms.

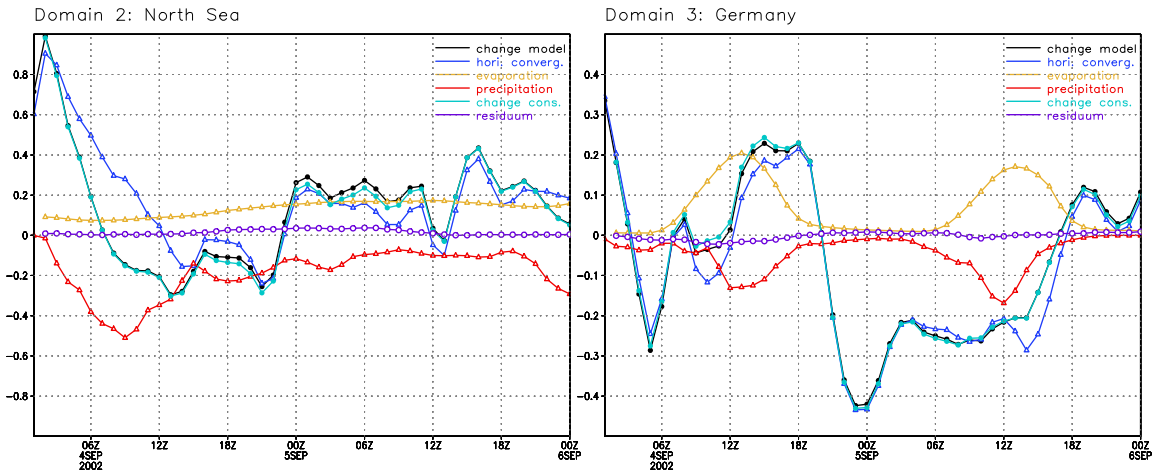

Figure 2: Normalized hourly area average water mass budget (mm/m^2 per hour) as a function of forecast time (hours). Left: subdomain 2 (North Sea). Right: subdomain 3 (Germany). The black line indicates the model predicted rate of change in water mass and the green line represents the 'exact' rate of change as calculated from (5) with the contributions from surface evaporation (yellow), precipitation (red) and horizontal total moisture convergence (-Div, blue). The residuum term is colored in purple.

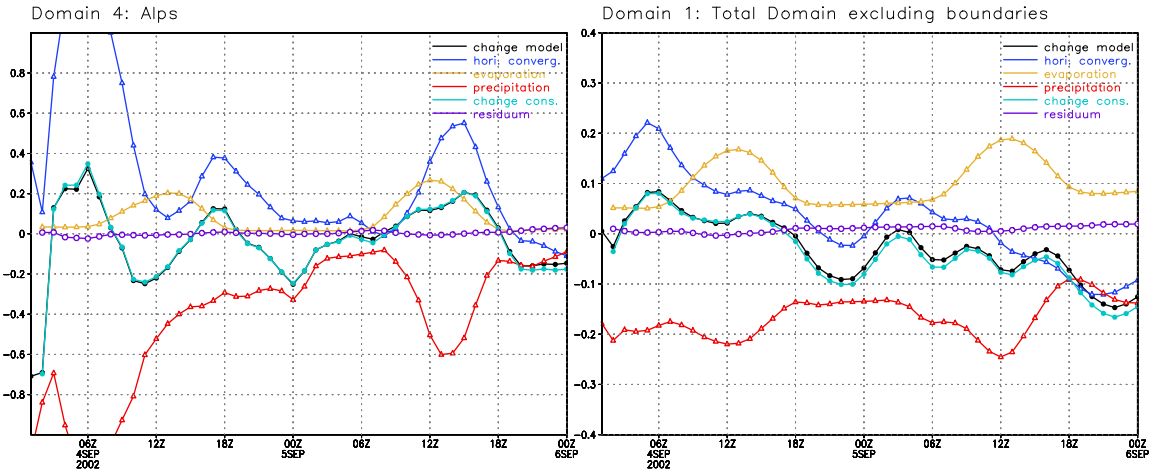

Figure 3: As in Fig. 3, but for subdomain 4 (Alps) and subdomain 1 (total domain excluding the relaxation zone).

A similar behaviour can be noticed in the water mass budgets for subdomain 3 (Germany). As for subdomain 2, the contributions from precipitation and evaporation balance approximately and the total change in water mass follows more or less the net inflow or outflow. Surface evaporation now has a clear diurnal cycle with a maximum around noon which is reflected in the area average precipitation. Bearing in mind the mass-flux closure condition in the Tiedtke convection parameterization, this indicates the presence of convection forced by surface evaporation. In contrast to subdomain 2, the maximum values for the residuum do now occur during daytime, most pronounced for the 9-15h forecast range. Also the net residuum has negative values, which means that the model looses water mass in this area.

The model behaviour is quite different in the Alpine region, where deep moist convection occurs during the integration (see Fig. 3, left). Evaporation from the ground has also a clear diurnal cycle as for subdomain 3, but now the mass loss due to precipitation is mainly balanced total moisture convergence – this reflects the moisture convergence closure of the convection scheme. The large amplitude of convergence and precipitation in the first 12 hours of integration is due to dynamic adaption of the unbalanced interpolated initial fields, which does not occur when starting from the LM nudging analysis. The value of the water mass residuum for the Alpine subdomain is surprisingly small. In a region, where we had expected the largest errors, the time-evolution of the model predicted water-mass change is almost identical to the diagnosed 'exact' budget (except for a short time period at about 5h and 46 h forecast time).

When looking at the water mass budget for the total domain excluding the lateral boundary zone (subdomain 1; see Fig. 3, right), we notice that precipitation is on the average approximately balanced by surface evaporation, and the total change in mass follows closely the total moisture inflow or outflow of the domain. Whereas the mass conservation appears to be very good during the first 18 hours of integration, the solution deteriorates in the following hours and the residuum becomes and stays slightly positive until the end of the forecast. This differs from the model behaviour in the smaller subdomains considered so far, where a nonzero residuum occurred only during relative short time periods. Thus, there must be other subdomains where the mass error behaviour is systematically different from the error evolution in the subdomains considered so far.

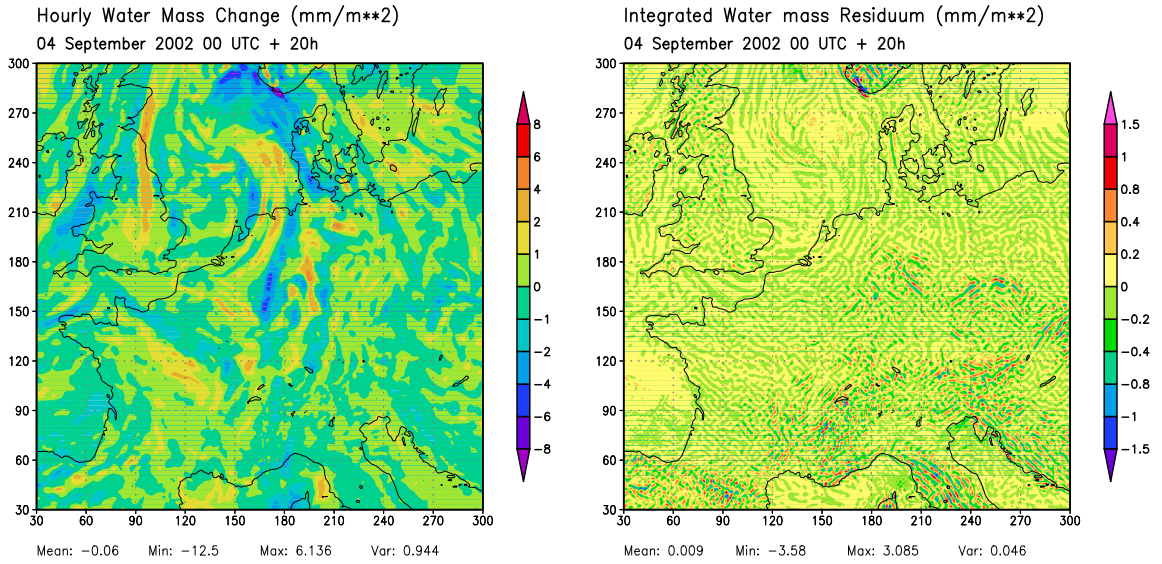

Figure 4: Left: Rate of change of the vertical integrated (column) water mass between 19-20 hours of forecast time. Right: Spatial distribution of the water mass residuum for the same time period.

Figure 4 (left) depicts the spatial distribution hourly change of vertically integrated water mass between 19 and 20 hours of forecast time. We notice larger local increases and decreases of atmospheric water in the vicinity of the northern low pressure system, which is associated with precipitation formation and transport caused by the frontal structures. Within the southern low pressure system, the change in water mass is much smaller. This indicates a good local balance of moisture convergence and convective precipitation – which is not surprising since this type of local balance is used as a closure condition to parameterize deep convection.

The distribution of the local error in the column water mass budget is also shown in Figure 4 (right). Over sea and flat terrain, the residual errors are close to zero with some small-scale structure. However, large local errors can be noticed over steep terrain (e.g Alps, Pyrenees, Apennin and east Adriatic coast) but a also over some mid-range mountain systems in Germany, France and Eastern Europe. Within these regions, the local error may be of the same order of magnitude as the vertically integrated change in water mass itself – which is a worrying result. Since these large errors do not show up in the area average budgets discussed above, they are presumably caused by model deficiencies related to horizontal transport: when the Div-terms are added over a subdomain, the horizontal fluxes will cancel in the inner area such that related errors will be counted only along the outer boundary of the subdomain. Nevertheless, the spatial error distribution clearly indicates that the LM model formulation is problematic over steep terrain.

Besides the use of terrain-following coordinates with corresponding errors in the discretization, the neglection of the diabatic heating term in the pressure equation (1) may be another possible reason for errors in the water mass budget (neglecting the heating term will mainly affect the total air density which is used in the definition of m_w). Recently, Bryan and Fritsch (2002) investigated the impact of this (and other) approximation to the basic thermodynamic equations on the simulation of a rising moist bubble. They noticed remarkable differences in the time evolution compared to their benchmark solution using the full non-approximated thermodynamic equations. However, for the simulation of more complex real cases, the differences between various thermodynamic model formulations revealed to be

much smaller. By evaluating a LM-simulation which retains the diabatic heating term in the pressure equation, we can in principle confirm this finding. The impact is relatively small and the structure of the water mass budget error is almost identical to the example in Fig. 4 (not shown): the area mean values as well as the maximum and minimum values of the residuum are reduced by about 10 - 15%. But even if the error reduction is relatively small, we will consider the inclusion of the heating term in a future version of LM for consistency reasons.

4 Conclusions

The case study considered here reveals that the column water budget of LM may behave quite different for various model subdomains, depending on the geographical location and the prevailing weather type. Of course, a number of additional cases must be evaluated in future to specify and confirm systematic differences. And also, a clear identification of causes for mass budget errors cannot be drawn by this type of diagnostic studies, but some useful hints may be obtained. The basic results form one case study considered so far are summarized below.

- The large-scale area-average budgets of water mass appears to be 'reasonable' for short-range NWP purposes since the magnitude of the area-average residuum is in general small compared to the absolute rate of change.
- Local imbalances in vertical columns can be much larger, especially over steep terrain – this indicates severe numerical problems related to the utilization of terrain-following coordinates.
- The inclusion of the diabatic heating term in the pressure equation improves the water mass budget slightly, but does not cure the principal problems.

A methodology to remove budget errors is the use of the basic continuity equations in flux form and conserving numerical schemes to calculate 3-d transport. This strategy is applied in the new WRF-model of the US meteorological community. However, a number of inherent accuracy problems related to terrain-following coordinates will remain (e.g. the discretization of the pressure gradient terms). Within COSMO, the LM_Z-project (see the paper *New Developments Concerning the Z-coordinate Version of LM* by J. Steppeler et al. in Section 9) tries to tackle the accuracy problem by developing a z-coordinate version of the model using a shaved-element finite-volume discretization.

5 References

Bryan, G. H. and J. M. Fritsch, 2002: A benchmark solution for moist nonhydrostatic numerical models. *Mon. Wea. Rev.*, 130, 2917–2928.

Wacker, U. and F. Herbert, 2003: Continuity equations as expressions for local balances of masses of cloudy air. Manuscript no. TEA301499 accepted for publication in *Tellus A*.